

The development of novel inhibitors of tumor necrosis factor- α (TNF- α) production based on substituted [5,5]-bicyclic pyrazolones

Matthew J. Laufersweiler,* Todd A. Brugel, Michael P. Clark, Adam Golebiowski, Roger G. Bookland, Steven K. Laughlin, Mark P. Sabat, Jennifer A. Townes, John C. VanRens, Biswanath De, Lily C. Hsieh, Sandra A. Heitmeyer, Karen Juergens, Kimberly K. Brown, Marlene J. Mekel, Richard L. Walter and Michael J. Janusz

Procter and Gamble Pharmaceuticals, Health Care Research Center, 8700 Mason-Montgomery Rd, Mason, OH 45040, USA

Received 25 March 2004; revised 2 June 2004; accepted 2 June 2004

Available online 19 June 2004

Abstract—Novel substituted [5,5]-bicyclic pyrazolones are presented as inhibitors of tumor necrosis factor- α (TNF- α) production. Many of these compounds show low nanomolar activity against lipopolysaccharide (LPS)-induced TNF- α production in THP-1 cells. This class of molecules was co-crystallized with mutated p38, and several analogs showed good oral bioavailability in the rat. Oral activity of these compounds in the rat iodoacetate model for osteoarthritis is discussed.

© 2004 Elsevier Ltd. All rights reserved.

The overexpression of cytokines, such as TNF- α and IL-1 β , has been implicated in a number of serious inflammatory disorders.¹ Consequently, agents that inhibit the production of TNF- α can decrease levels of these pro-inflammatory cytokines, and thereby reduce inflammation and prevent further tissue destruction in diseases such as rheumatoid arthritis (RA),² osteoarthritis (OA),³ and Crohn's disease.⁴ Thus, reduction of these cytokine levels has become an attractive goal in our efforts to discover disease modifying treatments for inflammatory disorders such as osteoarthritis. It is well documented that inhibition of p38 MAP kinase disrupts the cytokine synthesis pathway and results in decreased levels of pro-inflammatory cytokines leading to reduced inflammation and pain.¹ Early inhibitors of p38 (SB203580)⁵ typically contained a vicinal aryl-pyridinyl pharmacophore and were found to bind competitively with ATP in the p38 active site. It is known, however, that a number of homologous kinases, including c-jun N-terminal kinases (JNK's), disrupt this pathway as well

leading to similar therapeutic effects.⁶ With this in mind, our primary screening assay has involved measuring the level of TNF- α release from lipopolysaccharide (LPS)-induced THP-1 cells followed by second tier pharmacokinetic and in vivo studies.⁷ Herein we wish to report the development of a new class of [5,5]-bicyclic pyrazolones that inhibit the production of TNF- α . Studies have led to a series of orally active substituted bicyclic pyrazolones, **1** and **2**, useful in the inhibition of LPS induced TNF- α in THP-1 cells (Fig. 1).

Synthesis of the initial substituted bicyclic pyrazolones was accomplished in thirteen steps starting with *t*-Boc protection of benzyl carbamate (Scheme 1). Reaction with 3-chloro-2-chloromethylpropene followed by ozonolysis with reductive workup gave ketone **4**. Reduction with borane dimethylsulfide complex gave the hydroxy pyrazolidine. Alternatively, reductive amination with an amine leads to final compounds containing amine substituents (compound **11d**). Methylation of the hydroxyl followed by removal of the *t*-Boc protecting group under acidic conditions and acylation with 4-fluorophenylacetyl chloride gave intermediate **5**. Hydrolysis followed by acylation with 2-methylsulfanyl-pyrimidine-4-carbonyl chloride yielded the bis-acylated pyrazolidine **6**. Ring closure proceeded

Keywords: TNF- α ; Cytokine synthesis inhibition; Pyrazolones; p38; Kinases.

* Corresponding author. Tel.: +1-513-622-3135; fax: +1-513-622-3681; e-mail: laufersweiler.mj@pg.com

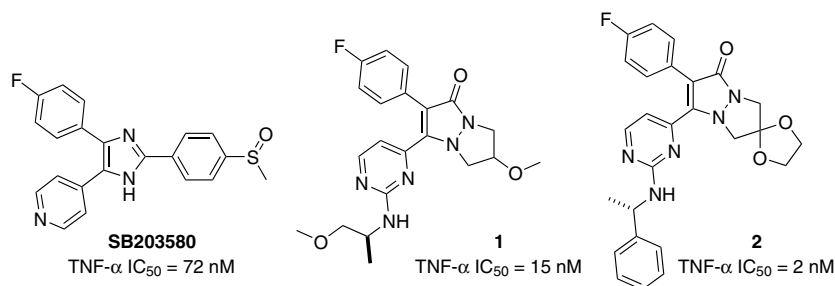
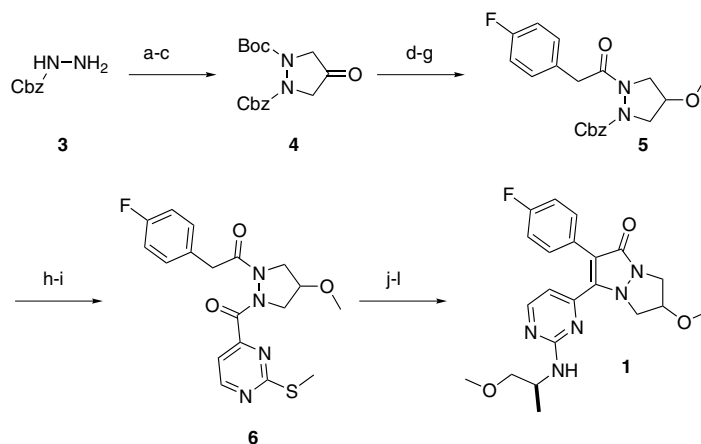


Figure 1. Selected inhibitors of TNF- α production.



Scheme 1. Reagents and conditions: (a) (Boc)₂O, N(Et)₃, CH₂Cl₂, 99%; (b) NaH, 3-chloro-2-chloromethylpropene, DMF, 96%; (c) O₃, CH₂Cl₂, DMS, 56%; (d) BH₃, DMS, 93%; (e) MeI, NaH, 97%; (f) MeOH, SOCl₂, 99%; (g) 4-fluorophenylacetyl chloride, CH₂Cl₂, H₂O, NaOH; (h) H₂, Pd/C, MeOH; (i) 2-methylsulfonyl-pyrimidine-4-carbonyl chloride, CH₂Cl₂, H₂O, NaOH, 83%, three steps; (j) NaH, DMF, -5 °C, 57%; (k) *m*-CPBA, CH₂Cl₂; (l) 2-methoxy-1-(*S*)-methylethyl amine, toluene, 90 °C, 45%, two steps.

through an intramolecular cyclocondensation to form the pyrazolone. This was followed by oxidation of the methyl sulfide and subsequent displacement with an appropriate nucleophile to give the final compounds (e.g., **1**).

All compounds were tested for the inhibition of TNF- α production using (LPS)-stimulated human monocytic cells (THP-1).⁸ Table 1 summarizes the potency of selected substituted bicyclic pyrazolones. A wide variety of substituents attached to the second ring of the bicyclic pyrazolones were well tolerated and compared favorably with previously published unsubstituted pyrazolones.⁷ Examination of the compounds with phenoxy substitution on the pyrimidine (**11d–i**) ring revealed no significant changes in potency with small changes in substitution on the bicyclic pyrazolone. This data suggests that there is no significant enzyme interaction with this portion of the molecules indicating that the substituents are solvent exposed in the enzyme pocket. This was confirmed by enzyme–inhibitor co-crystallization experiments discussed later.

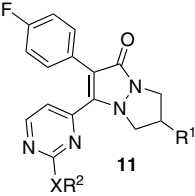
The diastereomers formed in this route were separable after the final step via chiral HPLC. It is interesting to note that in the case of compounds **1**, **11a**, and **11b** the absolute stereochemistry of the methoxy substituent seemed to make little difference, with the activity of the

racemate being equal to that of the individual diastereomers. This is believed to be due to the substituent being solvent exposed within the enzyme active site. In an effort to eliminate chiral centers in the molecules we turned our focus to the spiroketal [5,5]-bicyclic pyrazolones.

Synthesis of the spiroketal compounds was performed in nine steps from the pyrazolidine intermediate **7** (Scheme 2). Removal of the *t*-Boc protecting group followed by acylation with 4-fluorophenylacetyl chloride and subsequent ozonolysis gave key intermediate **8**. Ketal formation proceeded smoothly from the ketone with the appropriate diol under Dean–Stark conditions. This was followed by removal of the Cbz protecting group and acylation with 2-methylsulfonyl-pyrimidine-4-carbonyl chloride. Base mediated cyclocondensation, oxidation of the methyl sulfide and nucleophilic displacement yielded the final spiroketal [5,5]-bicyclic pyrazolones (e.g., **2**).

Potency of selected spiroketal [5,5]-bicyclic pyrazolones is summarized in Table 2. Examination of the data revealed that the potency seen in the five-membered dioxolane spirocyclic compounds was preserved in the six-membered dioxane spirocyclic compounds. Phenoxy pyrimidine substituents as well as amine substituents showed good activity, however the most active compounds (**2**, **12c**, **12j**) contained amine substituents on the

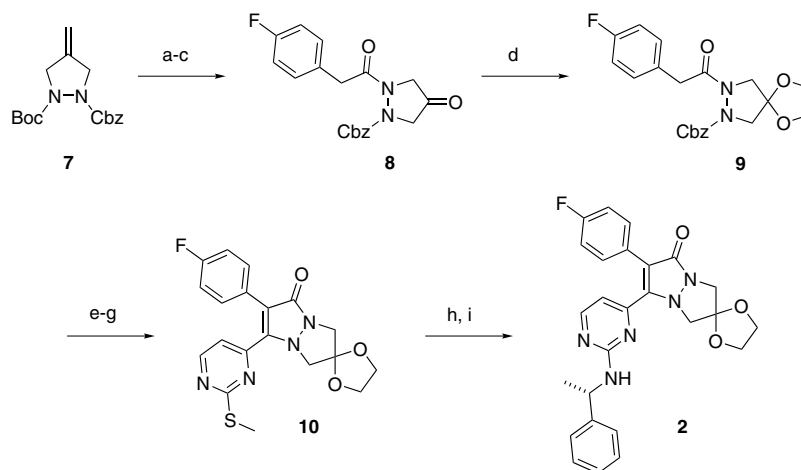
Table 1. Substituted bicyclic pyrazolones



| Compound | R ¹ | XR ² | TNF- α IC ₅₀ (nM) ^{a,b} |
|------------|---|---|--|
| 1 | –OMe (<i>rac</i>) | 2-Methoxy-1-(<i>S</i>)-methylethylamino | 15 |
| 11a | –OMe (<i>R</i>) | 2-Methoxy-1-(<i>S</i>)-methylethylamino | 20 |
| 11b | –OMe (<i>S</i>) | 2-Methoxy-1-(<i>S</i>)-methylethylamino | 13 |
| 11c | –OH | (<i>S</i>)-(-)- α -Methylbenzylamino | 5 |
| 11d | –N(Me) ₂ | Phenoxy | 177 |
| 11e |  | Phenoxy | 297 |
| 11f |  | Phenoxy | 327 |
| 11g |  | Phenoxy | 313 |
| 11h |  | Phenoxy | 500 |
| 11i |  | Phenoxy | 181 |

^a Standard deviations for whole cell assays were typically $\pm 30\%$ of the mean or less.

^b Cell viabilities were typically $>90\%$ at the IC₅₀.

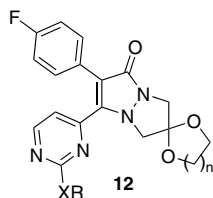


Scheme 2. Reagents and conditions: (a) MeOH, SOCl₂, 98%; (b) 4-fluorophenylacetyl chloride, CH₂Cl₂, H₂O, NaOH, 91%; (c) O₃, CH₂Cl₂, DMS, 78%; (d) ethylene glycol, *p*-TSA, toluene, reflux, 75%; (e) H₂, Pd/C, MeOH, 90%; (f) 2-methylsulfanyl-pyrimidine-4-carbonyl chloride, CH₂Cl₂, H₂O, NaOH, 82%; (g) NaH, DMF, –5 °C, 41%; (h) *m*-CPBA, CH₂Cl₂, 95%; (i) (*S*)-methylbenzyl amine, toluene, 90 °C, 98%.

pyrimidine ring. α -Methyl substitution on the amine substituents also tended to further improve the potency. However the benzylamine substituent (**12c**) maintained activity not typically seen without the chiral α -methyl substitution. This observation was further explored.

A summary of SAR developed around the benzylamine substituent on the pyrimidine ring is shown in Table 3. Substitution around the phenyl ring on the benzyl amine substituents had a significant impact on the activity of the molecules in the whole cell assay. A comparison of

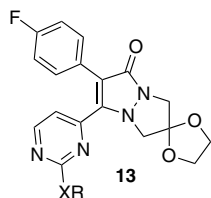
the fluoro substituted rings (**12e**, **13a–b**) reveals a trend in which activity increases from *para* substituted to *meta* substituted with *ortho* substitution showing the greatest potency. This trend was consistent among all substituents investigated. Comparison of the 2-fluoro, 2-trifluoromethyl, and 2-methyl substituents (**13b**, **13e**, **13h**) shows that the activity of these compounds remains fairly constant. This suggests that there is no significant electronic effect involved with substitution at this position and that the increased activity seen with the *ortho* substituted compounds is due to favorable steric

Table 2. Comparative activity of selected spiroketal [5,5]-bicyclic pyrazolone

| Compound | XR | <i>n</i> | TNF- α IC ₅₀ (nM) ^{a,b} |
|------------|---|----------|--|
| 12a | Phenoxy | 1 | 38 |
| 12b | Phenoxy | 2 | 69 |
| 12c | Benzylamino | 1 | 11 |
| 12d | Benzylamino | 2 | 31 |
| 12e | 4-Fluorobenzylamino | 1 | 290 |
| 12f | 4-Fluorobenzylamino | 2 | 630 |
| 2 | (<i>S</i>)-(-)- α -Methylbenzylamino | 1 | 2 |
| 12g | (<i>S</i>)-(-)- α -Methylbenzylamino | 2 | 12 |
| 12h | 2-Methoxy-1-(<i>S</i>)-methylethylamino | 1 | 36 |
| 12i | 2-Methoxy-1-(<i>S</i>)-methylethylamino | 2 | 36 |
| 12j | 2-Hydroxy-1,2-dimethyl-(<i>S</i>)-propylamino | 1 | 9 |

^a Standard deviations for whole cell assays were typically $\pm 30\%$ of the mean or less.

^b Cell viabilities were typically $>90\%$ at the IC₅₀.

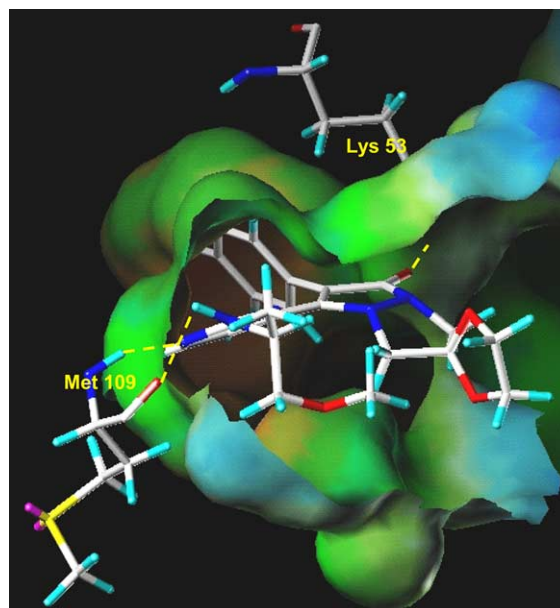
Table 3. Comparative activity of selected benzylamino pyrimidine spiroketal [5,5]-bicyclic pyrazolones

| Compound | XR | TNF- α IC ₅₀ (nM) ^{a,b} |
|------------|------------------------------|--|
| 12c | Benzylamino | 11 |
| 12e | 4-Fluorobenzylamino | 290 |
| 13a | 3-Fluorobenzylamino | 13 |
| 13b | 2-Fluorobenzylamino | 8 |
| 13c | 4-Trifluoromethylbenzylamino | 1000 |
| 13d | 3-Trifluoromethylbenzylamino | 197 |
| 13e | 2-Trifluoromethylbenzylamino | 17 |
| 13f | 4-Methylbenzylamino | 293 |
| 13g | 3-Methylbenzylamino | 40 |
| 13h | 2-Methylbenzylamino | 19 |
| 13i | 4-Aminobenzylamino | 161 |
| 13j | 2-Aminobenzylamino | 101 |
| 13k | (Pyridin-4-ylmethyl)-amino | 1000 |
| 13l | (Pyridin-3-ylmethyl)-amino | 427 |
| 13m | (Pyridin-2-ylmethyl)-amino | 148 |

^a Standard deviations for whole cell assays were typically $\pm 30\%$ of the mean or less.

^b Cell viabilities were typically $>90\%$ at the IC₅₀.

interactions. Hydrophilic substituents placed in the *ortho* position, such as compound **13j**, lower activity. Additionally the 4-aminobenzylamine (**13i**) is more active than the corresponding 4-substituted benzylamines. Replacement of the phenyl ring with a pyridine ring (**13k–m**) also seems to have a negative effect on the whole cell activity of these compounds.

**Figure 2.** Compound **12h** bound in the active site of mutated p38.

Co-crystallization of compound **12h** with mutated p38 showed how these compounds bind in the enzyme active site (Fig. 2).¹¹ A hydrogen bond between the backbone amide N–H of Met-109 and the pyrimidine ring was observed as well as a second hydrogen bond between the N–H of the amine substituent and the backbone carbonyl of Met-109. This second hydrogen bond may account for the increased potency seen with amine substituted pyrimidine rings within this series. The pyrazolone carbonyl forms a third hydrogen bond with Lys-53 while the fluorophenyl ring resides in the Thr-106 hydrophobic pocket. As discussed earlier, the substituent on the bicyclic pyrazolone is solvent exposed. This allowed for optimization of the physical and

Table 4. Pharmacokinetic properties and in vivo data of selected compounds

| | TNF- α IC ₅₀ (nM) | Solubility (mg/mL) | <i>t</i> _{1/2} (h) | %F | RIA (% reduction) ^a |
|------------|--|-----------------------|-----------------------------|------|-----------------------------------|
| 1 | 15 | 1.6 | 1.2 | 52.2 | 28 |
| 2 | 2 | 0.04 | 0.7 | 17.2 | 27 |
| 12h | 36 | 0.7 | 1.4 | 22.4 | 17 |
| 12j | 9 | 0.81 | 2.1 | 22.3 | 18 |

^a Percent reduction in joint damage as compared to vehicle control at a dose of 25 mg/kg. Statistically significant at *P* < 0.05.

pharmacokinetic properties of these molecules without sacrificing potency.

Examination of the pharmacokinetics of selected compounds prompted in vivo testing of three compounds (Table 4). Compound **1** showed excellent solubility with good bioavailability and an acceptable half-life in the rat. Compound **2** was one of the most active compounds tested, however it had very poor solubility, a fairly short half-life, and only moderate bioavailability. Compound **12h** showed significant improvement in solubility, half-life, and bioavailability however it was less active than other compounds. Finally, compound **12j** had excellent whole cell activity (IC₅₀ = 9 nM), good solubility, the longest half-life among the compounds tested, and acceptable bioavailability. Compounds **1**, **2**, **12j**, and **12h** were tested in the rat iodoacetate (RIA) model for osteoarthritis¹⁵ and showed positive oral efficacy at a dose of 25 mg/kg.

In summary, we have reported a novel series of substituted bicyclic pyrazolones that inhibit the release of TNF- α in monocytic cells (THP-1). Efforts to eliminate the chiral center in the substituted bicyclic pyrazolones led to the development of spiroketal analogs. Excellent potency was observed in both the dioxolane spiroketal and the dioxane spiroketal with the dioxolane compounds showing slightly higher potency. The potency was preserved with benzyl amine substituents on the pyrimidine ring even when no α -methyl chiral center was present. We observed good oral bioavailability within the series and described four compounds that displayed oral efficacy (25 mg/kg) in the rat iodoacetate in vivo model for osteoarthritis.

Acknowledgements

We are grateful to: A. L. Roe, D. C. Ackley, A. M. Walter, C. R. Dietsch, and D. M. Bornes for pharmacokinetic data; A. Greib for chiral HPLC separation; and M. Buchalova for formulations and solubility data.

References and notes

- For recent reviews, see: (a) Palladino, M. A.; Bahjat, F. R.; Theodorakis, E. A.; Moldawer, L. L. *Nat. Rev. Drug Discovery* **2003**, *2*, 736–746; (b) Baugh, J. A.; Bucala, R. *Curr. Opin. Drug Discovery Dev.* **2001**, *4*, 635–650; (c) Adams, J. L.; Badger, A. M.; Kumar, S.; Lee, J. C. In

- Progress in Medicinal Chemistry*; King, F. D., Oxford, A. W., Eds.; Elsevier: Amsterdam, 2001; Vol. 38, pp 1–60; (d) Chen, Z.; Gibson, T. B.; Robinson, F.; Silvestro, L.; Pearson, G.; Xu, B.-e.; Wright, A.; Vanderbilt, C.; Cobb, M. H. *Chem. Rev.* **2001**, *101*, 2449–2476.
- (a) Smolen, J. S.; Seiner, G. *Nat. Rev. Drug Discovery* **2003**, *2*, 473; (b) Pearce, G. J.; Chikanza, I. C. *BioDrugs* **2001**, *15*, 139–149; (c) Moreland, L. W.; Baumgartner, S. W.; Schiff, M. H.; Tindall, E. A.; Fleisenmann, R. M.; Weaver, A. L.; Ettliger, R. E.; Cohen, S.; Koupman, W. J.; Mohler, K.; Widmer, M. B.; Blosch, C. M. *N. Engl. J. Med.* **1997**, *337*, 141–153.
 - (a) Brennan, F. M.; Feldman, M. *Curr. Opin. Immunol.* **1996**, *8*, 872–877; (b) Camussi, G.; Lupia, E. *Drugs* **1998**, *55*, 613–620.
 - Rutgeerts, P.; D'Haens, G.; Targan, S.; Vasiliaskas, E.; Hanauer, S. B.; Present, D. H.; Mayer, L.; Van Hozegand, R. A.; Braakman, T.; DeWoody, K. L.; Schaible, T. F.; Van Deventer, S. J. H. *Gastroenterology* **1999**, *117*, 761–769.
 - Gallagher, T. F.; Fier-Thompson, S. M.; Garigipati, R. S.; Sorenson, M. E.; Smietana, J. M.; Lee, D.; Bender, P. E.; Lee, J. C.; Laydon, J. T.; Chabot-Fletcher, M. C.; Breton, J. J.; Adams, J. L. *Bioorg. Med. Chem. Lett.* **1995**, *5*, 1171–1174.
 - (a) Wilson, K. P.; McCaffrey, P. G.; Hsiao, K.; Pazhanisamy, S.; Galullo, V.; Bemis, G. W.; Fitzgibbon, M. J.; Caron, P. R.; Murcko, M. A.; Su, M. S. *Chem. Biol.* **1997**, *4*, 423–431; (b) Wang, Z.; Canagarajah, B. J.; Boehm, J. C.; Kassisa, S.; Cobb, M. H.; Young, P. R.; Abdel-Meguid, S.; Adams, J. L.; Goldsmith, E. J. *Structure* **1998**, *6*, 1117–1128; (c) Smolen, J. S.; Steiner, G. *Nat. Rev. Drug Discovery* **2003**, *2*, 473–488.
 - Clark, M. P.; Laughlin, S. K.; Laufersweiler, M. J.; Bookland, R. G.; Brugel, T. A.; Golebiowski, A.; Sabat, M. P.; Townes, J. A.; VanRens, J. C.; Djung, J. F.; Natchus, M. G.; De, B.; Hsieh, L. C.; Xu, S. C.; Walter, R. L.; Mekel, M. J.; Heitmeyer, S. A.; Brown, K. K.; Juergens, K.; Taiwo, Y. T.; Janusz, M. J. *J. Med. Chem.* **2004**, *47*, 2724–2727.
 - Duplicate cultures of human monocytic cells (THP-1)⁹ cells (2.0 × 10⁵/well) were incubated for 15 min in the presence or absence of various concentrations of inhibitor before the stimulation of cytokine release by the addition of lipopolysaccharide (LPS, 2 μg/mL). The amount of TNF- α released was measured 4 h later using an ELISA (R & D Systems, Minneapolis, MN). The viability of the cells after the 4 h incubation was measured using MTS assay¹⁰ (Promega Co., Madison, WI).
 - Mohler, K. M.; Sleath, P. R.; Fitzner, J. N.; Cerretti, D. P.; Alderson, M.; Kerwar, S. S.; Torrance, D. S.; Otten-Evans, C.; Greenstreet, T.; Weerawarna, K.; Kronhelm, S. R.; Petersen, M.; Gerhart, M.; Kozlosky, C. J.; March, C. J.; Black, R. A. *Nature* **1994**, *370*, 218–220.
 - Barltrop, J. A.; Owen, T. C.; Cory, A. H.; Cory, J. G. *Bioorg. Med. Chem. Lett.* **1991**, *1*, 611–614.
 - The mutated p38 α herein described is a double mutant (S180A, Y182F) of murine p38 α .¹² The mutant enzyme cannot be phosphorylated and, therefore, it is not competent for activation. Protein expression and purification were carried out as previously described for the murine enzyme.¹³ For crystallization, mutated p38 α was incubated overnight (12–16 h) with 1 mM compound. Co-crystals were grown by hanging drop vapor diffusion using PEG as a precipitating agent and overall protocols similar to those previously described for the human enzyme.¹⁴ Crystals typically diffracted to 1.9 Å resolution and were of the previously reported space group: *P*₂₁₂₁; *a* = 65.2 Å, *b* = 74.6 Å, *c* = 78.1 Å (4'). X-ray data were collected at

- beamline 17-BM in the facilities of the Industrial Macromolecular Crystallography Association Collaborative Access Team (IMCA-CAT) at the Advanced Photon Source. These facilities are supported by the companies of the Industrial Macromolecular Crystallography Association through a contract with Illinois Institute of Technology (IIT), executed through IIT's Center for Synchrotron Radiation Research and Instrumentation. Use of the Advanced Photon Source was supported by the U. S. Department of Energy, Basic Energy Sciences, Office of Science, under Contract No. W-31-109-Eng-38.
12. Han, J.; Lee, J. D.; Bibbs, L.; Ulevitch, R. J. *Science* **1994**, *265*, 808–811.
 13. Wang, Z.; Harkins, P. C.; Ulevitch, R. J.; Han, J.; Cobb, M. H.; Goldsmith, E. J. *Proc. Natl. Acad. Sci. U.S.A.* **1997**, *94*, 2327–2332.
 14. Pav, S.; Whit, D. M.; Rogers, S.; Crane, K. M.; Cywin, C. L.; Davidson, W.; Hopkins, J.; Brown, M. L.; Pargellis, C. A.; Tong, L. *Protein Sci.* **1997**, *6*, 242–245.
 15. Sprague–Dawley male rats (200–225 g) from Harlan (Oregon, WI) under anesthesia were injected in the patellar ligament region of the left leg (flexed 90° at the knee) with 20 μ L of a 10 mg/mL concentration of monosodium iodoacetate (IA) (Aldrich Chemical, Milwaukee, WI). Animals (groups of 15) were dosed for 7 days BID (~every 12 h) with the potential inhibitor (25 mg/kg) or vehicle (2.5 mL/kg). Animals were sacrificed on day 22 and the left joint was disarticulated and fixed in 10% formalin for 24–48 h prior to capturing the image. An image of the tibial cartilage surface was captured using an Optimas (Optimas, Media Cybernetics LP, Silver Springs, MA) image analysis system. Three independent observers assessed the damage in a blinded manner using a scale of 0–4 of increasing severity (0 = normal; 4 = maximum severity).¹⁶
 16. Guingamp, C.; Gegout-Pottier, P.; Philippe, L.; Terlain, B.; Netter, P.; Gillet, P. *Arthritis Rheum* **1997**, *40*, 1670.